SANDIA REPORT

SAND95–2353 • UC–400
Unlimited Release
Printed October 1995

Discharge Rates of Porous Carbon Double Layer Capacitors

Erhard T. Eisenmann

Prepared by
Sandia National Laboratories
Albuquerque, New Mexico 87185 and Livermore, California 94550
for the United States Department of Energy
under Contract DE-AC04-94AL85000

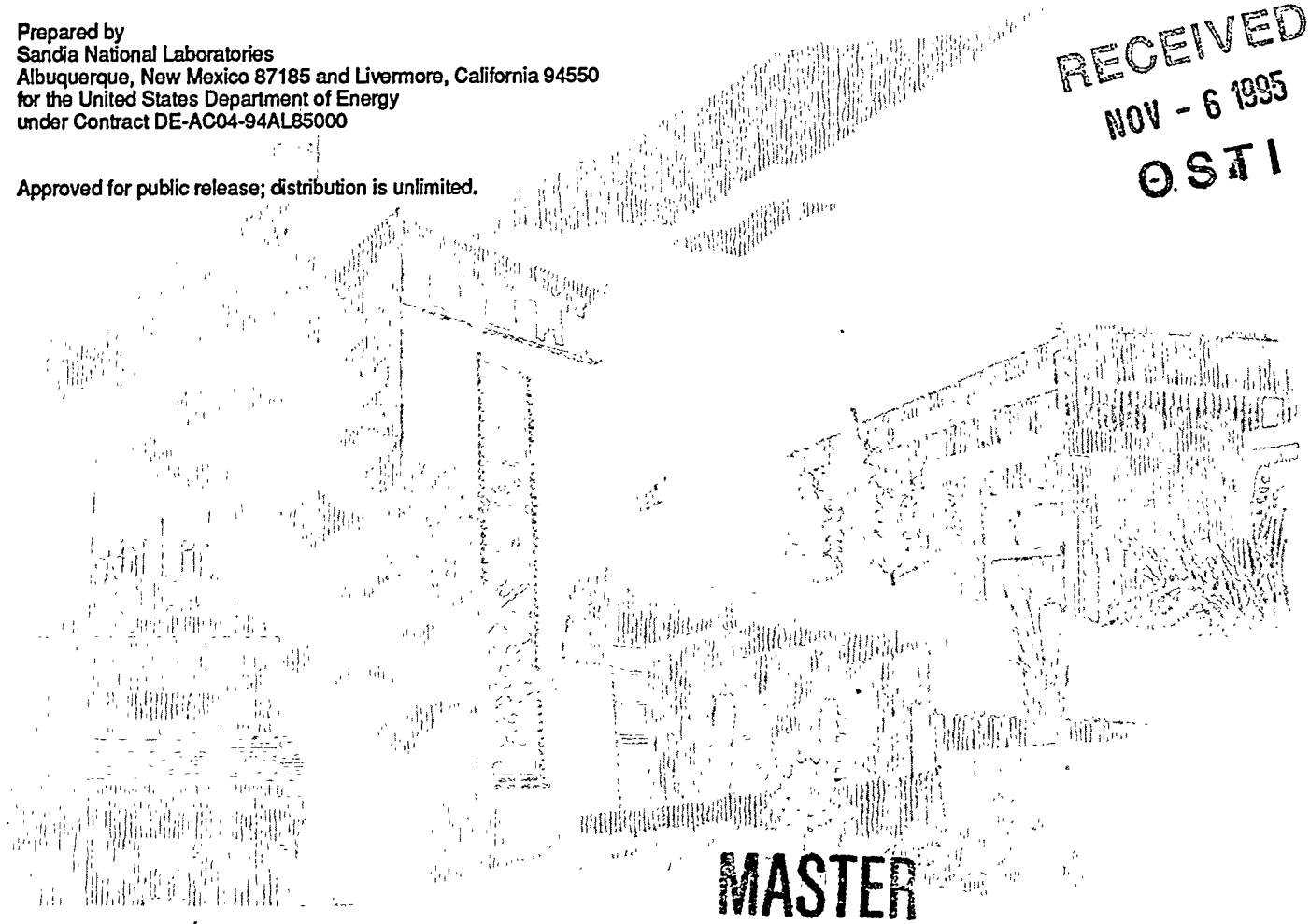

Issued by Sandia National Laboratories, operated for the United States Department of Energy by Sandia Corporation.

Available to DOE and DOE contractors from
Office of Scientific and Technical Information
PO Box 62
Oak Ridge, TN 37831

Prices available from (615) 576-8401, FTS 626-8401

Available to the public from
National Technical Information Service
US Department of Commerce
5285 Port Royal Rd
Springfield, VA 22161

NTIS price codes
Printed copy: A03
Microfiche copy: A01

SAND95-2353
Unlimited Release
Printed October 1995

Distribution
Category UC-400

Discharge Rates of Porous Carbon Double Layer Capacitors

Erhard T. Eisenmann
Battery Research Department
Sandia National Laboratories
Albuquerque, NM 87185

Abstract

Double layer capacitors with porous carbon electrodes have very low frequency response limits and correspondingly low charge-discharge rates. Impedance measurements of various commercial double layer capacitors and of carbon electrodes prepared from selected precursor materials were found to yield similar, yet subtly different characteristics. Through modeling with the traditional transmission line equivalent circuit for porous electrodes, a resistive layer can be identified, which forms on carbon films during carbonization and survives the activation procedure. A method for determining the power-to-energy ratio of electrochemical capacitors has been developed. These findings help define new ways for optimizing the properties of double layer capacitors.

Contents

Figures

Discharge Rates of Porous Carbon Double Layer Capacitors

Introduction

Double layer capacitors (DLCs) have higher energy storage densities than conventional electrolytic capacitors, but batteries still store orders of magnitude more energy. Capacitors, however, have greater power density than batteries, which is the rationale behind the proposal to use DLCs as load-leveling devices for batteries, for example in electric vehicles. The charge-discharge cycle life of DLCs usually surpasses that of batteries, provided that their energy storing mechanism is predominantly non-faradaic. Capacitive energy storage in load-leveled pulse power systems should have energy and power densities[1] of 15 Wh/kg and 1500 W/kg, respectively, and should be limited to less than 10% of the total system weight. Major difficulties have been encountered in the attempt to achieve these energy and power densities with pure, electrostatic DLCs in, both, aqueous and nonaqueous systems.[2] Aqueous systems have a maximum voltage of 1.2 V, and would require the impossible combination of exorbitant surface areas with micropores whose size is comparable to the double layer thickness. Nonaqueous electrolytes have relatively high resistance, lack pore accessibility and tend to break down under polarization. When suitably composed, nonaqueous systems seem to offer high levels of pseudocapacitance, as demonstrated by tests on capacitors built for DOE by Maxwell Laboratories.[3] However, the reliance on faradaic processes make these devices similar to batteries, and their charge-discharge cycle life remains yet to be seen.

All capacitors that either have porous electrodes or rely on charge transfer reactions are potentially limited in their charge and discharge rates. DLCs with porous electrodes represent a distributed network of RC components, analogous to ac transmission lines, while pseudocapacitors may depend on slow charge transfer reactions and diffusion processes. This study addressed the frequency dependence of various commercial DLCs and of carbon electrodes prepared from selected precursor materials. Various characteristics are modeled with the transmission line equivalent circuit, thus providing insight into some of the peculiarities of electrochemical capacitors.

Impedance Measurements of Commercial Double Layer Capacitors

DLCs from several commercial sources were subjected to impedance tests, using a Solartron (Schlumberger) 1255 HF Frequency Response Analyzer in combination with an EG&G Princeton Applied Research Potentiostat Model 273, both controlled by a data acquisition system. The potentiostat had a tendency to oscillate, which limited the useful measuring range to below 1000 Hz, or even lower for very high capacitances. Figure 1 presents selected measurements with the reactance plotted versus the resistance. Although there is no evidence of arcs that would suggest faradaic processes, varying slopes are characteristic of all data sets. This behavior is at variance with what ideally is expected for

a capacitor - resistor combination. For example, 0.318 F in series with 10 Ω, when tested over a frequency range of 0.01 - ∞, should have a response as shown by the vertical line, located at the abscissa value of 10.

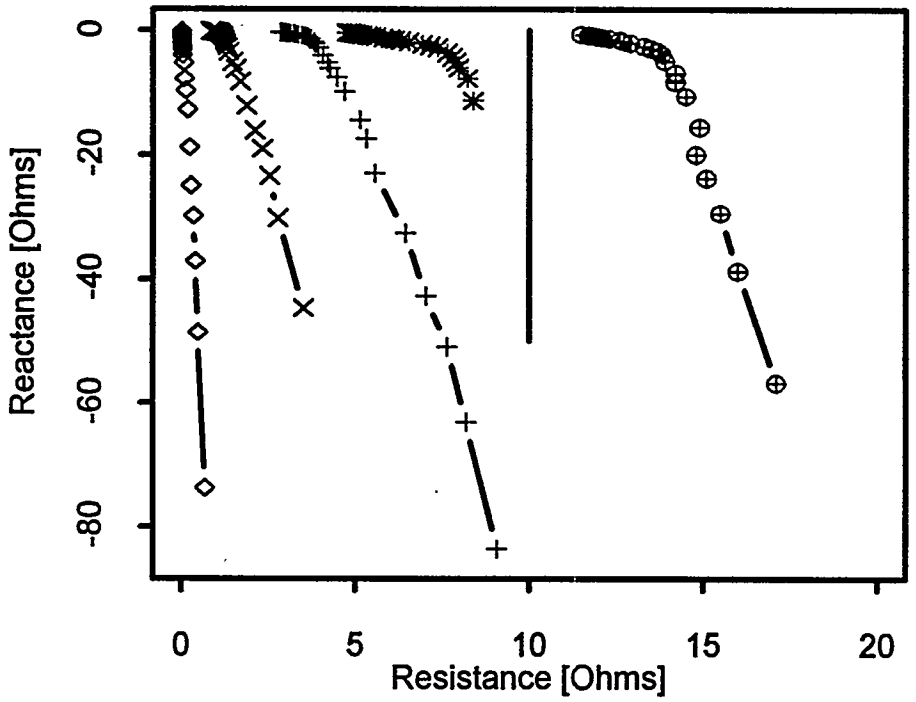

Figure 1: Complex impedance plots for commercial capacitors.

Impedance plots present difficulties in their interpretation whenever multiple factors affect the reactance, as seems to be the case for the data in Figure 1. Alternative plotting schemes were explored, therefore, as will be discussed in the following.

Equivalent Circuit for DLCs

The modeling approach of this investigation emulates the work by Keiser, Beccu and Gutjahr,[4] except for not making the assumption of cylindrical pores and, therefore, precluding a closed-form mathematical solution. Numerical calculations were carried out, instead, with a recursive formula similar to the one employed by these authors, on the premise that the ac response of a porous electrode equals that of a transmission line. This characterization of the electrode merely states that any change in charge at the solid-liquid interface advances from the surface of the porous body to its interior. Figure 2 illustrates the proposed equivalent circuit, where capacitors C(1), C(2), ...C(n) stand for equal capacitance increments, which in turn correspond to equal increments of accessible pore area. Being all switched in parallel, their sum equals the dc capacitance, C, of the circuit. Equal resistors, Rp, appear parallel to the capacitors C(1)-C(n) to represent electron transfer reactions. If there is no charge transfer, as was assumed because this study addresses electrostatic DLCs, Rp approaches infinity. The resistors R(1), R(2),...R(n)

symbolize resistance increments of the electrolyte in the pores, but may also include resistance contributions from the electrode material. Progressing from R(1) to R(n) corresponds to the penetration from the surface to the bulk of the porous structure. Variations in the porous body can be accounted for in the model by switching several or many transmission line circuits in parallel. Values of R, Rp and C may be combined to calculate the complex impedance of the circuit, according to textbook formulas.

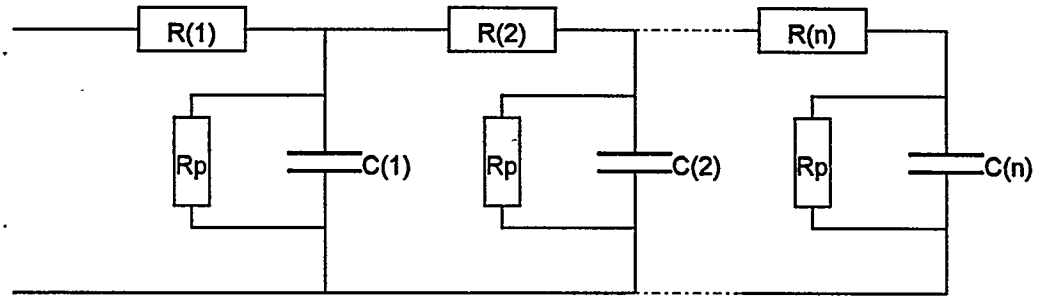

Figure 2: Equivalent circuit for porous electrodes.

For illustration purposes in the following discussions the capacity, C, as derived from the reactance, $-i/(\omega C)$, is the preferred parameter for the creation of capacitance plots versus the frequency. Impedance calculations for the equivalent circuit allow to describe in general terms how the capacitance varies as a function of the circuit elements and the frequency, as follows.

1. If $C = C(1)+C(2)+...C(n) > 0$, $R(1) > 0$, $R(2)$ to $R(n) = 0$ and $Rp = \infty$ then there is no dependence of the capacitance on the frequency.
2. If the conditions of case 1 are modified so that $R(1) = R(2) = ... = R(n) > 0$ then the capacitance will be constant below a critical frequency and then decrease with a slope of -0.5 in a double logarithmic plot, to reach a new capacitance level of C/n.
3. If the conditions of case 2 are changed so that the resistors R(i) are a function of their position in the transmission line then the capacitance decreases with frequency at a rate that may be greater or smaller than in case 2, but reaches the same final capacitance level of C/n.
4. If Rp is comparable to the resistors R(i) then the capacitance at low frequency may exceed the value of C and approach it with increasing frequency.

Impedance measurements of DLCs usually are consistent with the above case 3. Figures 3 and 4 have been prepared, therefore, to illustrate how the positional distribution of the resistors, R(i), affects the shape of the capacitance response curve. Comparatively high resistance values for a few low index numbers, i, lead to slopes steeper than -0.5. A few high resistance values at high index numbers (curve 4 in Figure 3), however, have no effect and the slope approaches -0.5.

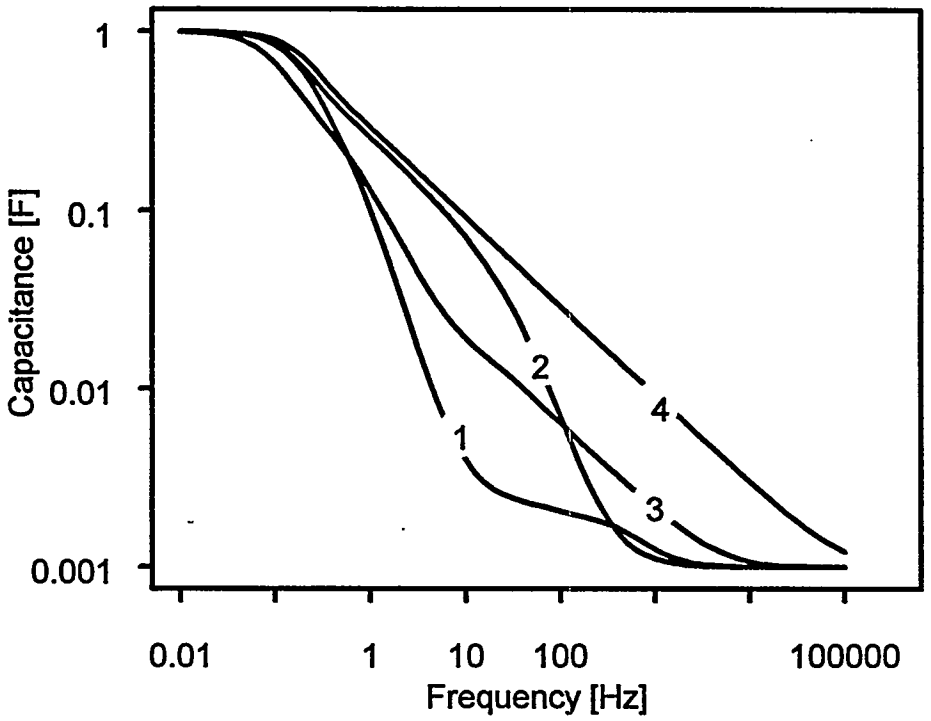

Figure 3: Capacitance plot for equivalent circuit with C = 1 Farad, Rp = 10^9 Ohms, n = 1000 and R(i) as shown by the distributions in Figure 4. The R(i)s for curve 4 are identical with those for curve 1 in reverse order.

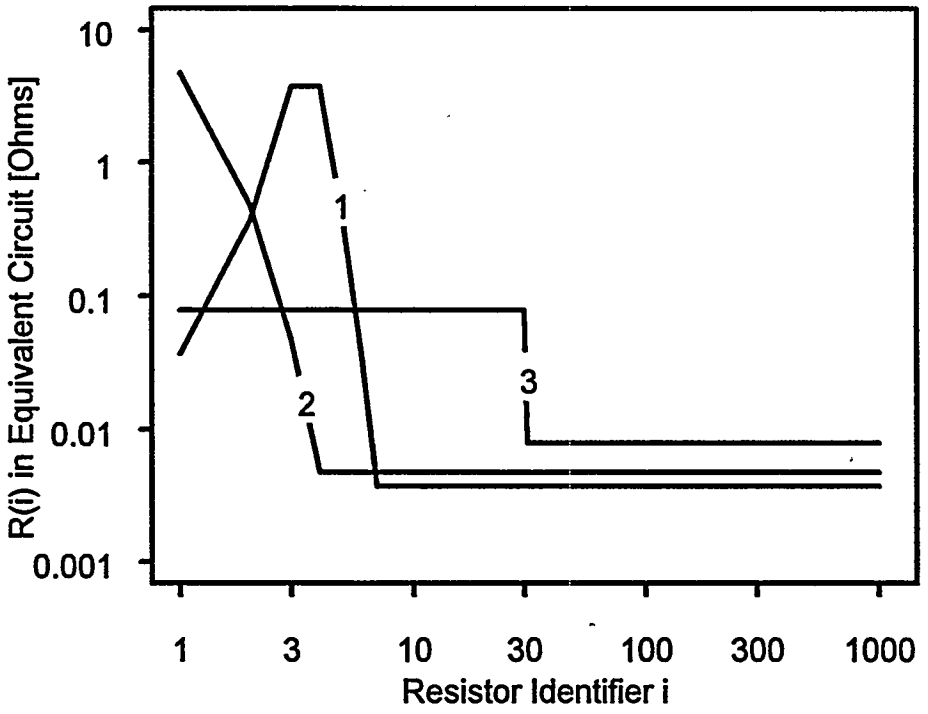

Figure 4: Resistance distributions used in the equivalent circuit to generate the curves in Figure 3.

Frequency Response of DLCs

Figure 5 shows the response curves for five DLCs and one electrolytic capacitor (Sprague). All test results were as expected, with the DLCs showing a plateau over some frequency range, followed by a decline that approaches a slope of -0.5, while the electrolytic capacitor showed no frequency dependence. Four additional Maxcap devices with nominal capacitance values of 0.047, 0.1, 0.22 and 0.47 F behaved such that their response curve could accurately be superimposed over that of the 1 F capacitor by translation along the ordinate in Figure 5.

An equivalent, but visually more discriminating diagram can be generated on the basis of the absolute magnitude of the impedance,

$$|Z| = \{Z_{real}^2 + Z_{imag}^2\}^{1/2} \ [\Omega]. \qquad (1)$$

Plotting the capacitance data of Figure 5 against this variable leads to Figure 6, which shows sharp capacitance cutoffs. This phenomenon has its cause in the distributed capacitance and series resistance of electrochemical capacitors. As the impedance decreases with increasing frequency a point is reached where the charge-discharge processes in the depth of the porous structure are sufficiently out of phase with those at the surface to become negligible. No such effect is evident for the electrolytic capacitor (Sprague). Figure 7 shows the same data plotted versus the phase angle and suggests that a phase angle of 90 degrees yields the best performance. This is again exemplified by the electrolytic capacitor, for which the range of angles is exceptionally narrow.

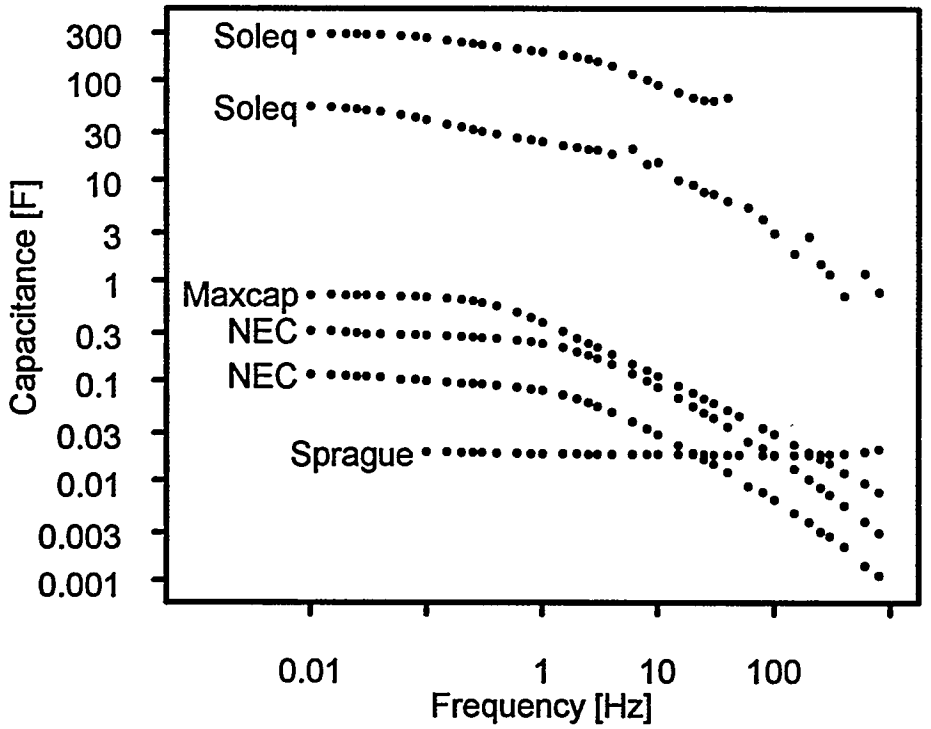

Figure 5: Frequency dependence of various commercial capacitors.

One may equate the cutoff impedance in Figure 6 with the equivalent series resistance (R_s) of a capacitor. If a capacitor were shorted, all energy would dissipate at the fastest possible rate with a time constant of

$$t_{cutoff} = R_s C \ [sec]. \tag{2}$$

The voltage and current at the start of the discharge, and therefore, the power P, depend on the energy, E, stored in the capacitor such that

$$P / E = 2 / t_{cutoff}[1/sec]. \tag{3}$$

It is the physical layout of the capacitor and the materials used for its construction that control P/E, while the actual capacitance and maximum charging voltage do not enter as

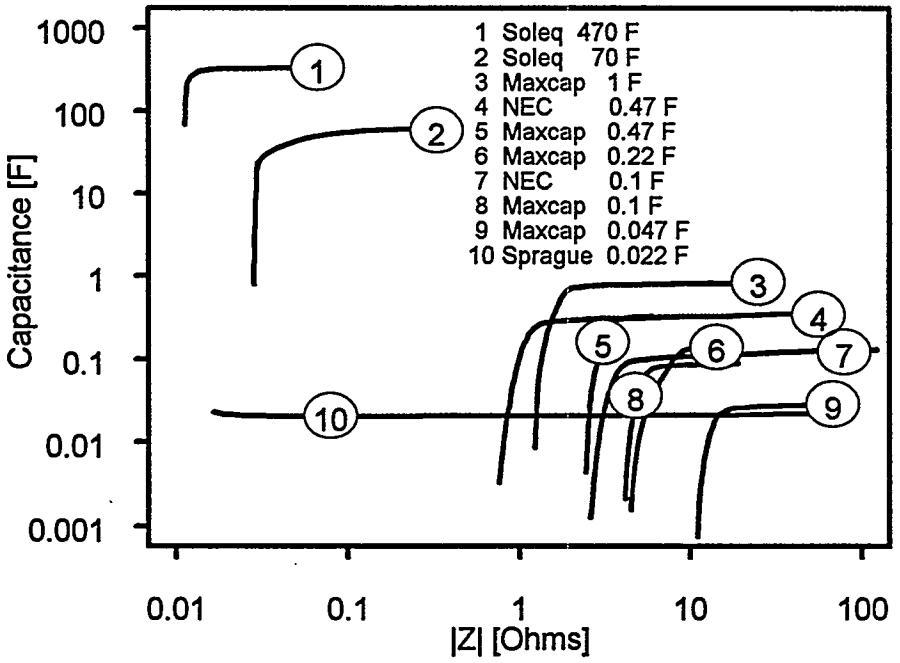

Figure 6: Determination of impedance limits for commercial capacitors.

variables. Equation (3) thus enables the comparison of capacitors and materials in terms of t_{cutoff}. DOE goals call for a P/E ratio of 0.0278 sec^{-1}, or a cutoff time of 72 seconds. Evidently, the power at the time the short circuit is established is

$$P = R_s V^2 = C V^2 / t_{cutoff} \ [W], \tag{4}$$

where C = capacitance and V = voltage at the start of the discharge.

Adding an external (load) resistor, R_l, to the transmission line equivalent circuit causes the cutoff impedance to increase and to become steeper. Therefore, measuring the

impedance of capacitors, with the appropriate load resistor in series, yields their power ratings according to equation (4). For example, a 1 F capacitor that is charged to 1 V will, at the start of its discharge through a 1 Ω resistor deliver 1 W, provided that $R_s << 1$. This latter condition actually decides, if the expected power can be delivered or not.

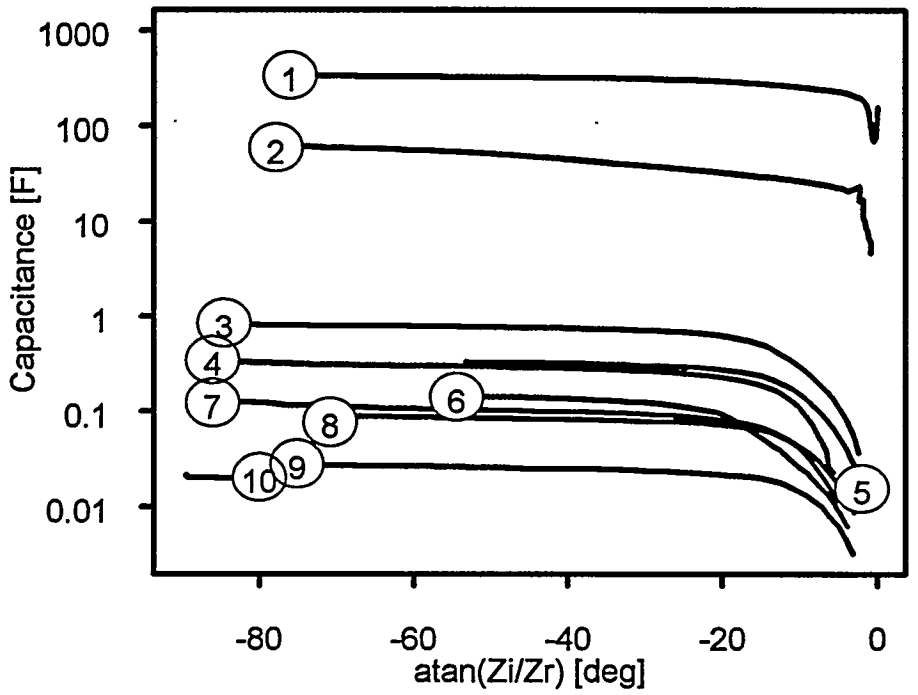

Figure 7: Capacitance data for commercial capacitors in dependence of the phase angle as calculated from the imaginary and real parts of the impedance Z.

Frequency Response of Porous Carbon Capacitor Materials

Previous investigations showed that activated, polyimide-derived carbon films[5] reach higher specific capacitance levels than any other carbon material. However, because of their comparatively high density, these carbons were suspected of having a higher equivalent resistance than other electrode materials. Samples with increasing surface accessibility, as prepared by stepwise activation, were measured in a three-electrode cell, using 1 M sulfuric acid electrolyte and a bias of 0.3 V vs. SHE. Figure 8 summarizes the results with the example of four activation stages, omitting additional data sets in favor of improved visual clarity.

Two features of these response curves differ from those of the commercial DLCs:

1. The slopes in the 10 to 300 Hz range are steeper, about -0.8 versus -0.5.
2. Only the maximally activated sample produces a plateau. The other samples show a segment with a slope between -0.2 and -0.3, which shifts to higher capacitance levels as the activation progresses.

This behavior is consistent with the existence of a resistive layer at the surface of the carbon samples, as previously demonstrated for the equivalent circuit, which yielded slopes steeper than -0.5 when low-indexed resistors assumed high values. This resistive layer may be identical with the low-porosity envelope of certain polymer-derived porous carbons, which W. R. Even[6] detected in studies with the transmission electron microscope. The shapes of the response curves were modeled with the resistance distributions in Figure 9, yielding the lines that have been drawn through the points of Figure 8. These lines serve for visual comparison, only, and represent no statistical fit to the data. It should be noted, however, that the very high resistance values for the transmission line lead to impedances with the real part not exceeding 30Ω, thus placing them within realistic bounds.

Figure 10 contains a plot of the capacitance versus |Z| for the polyimide-derived carbons. Compared with Figure 6, the capacitance cutoff for the carbon films is more gradual than for the commercial capacitors, except for the maximally activated sample. Accordingly, the cutoff impedance for these incompletely activated samples is more appropriately determined as a range, which causes the cutoff time (equation 2) to deteriorate into a range as well. Similar circumstances exist for another carbon film material, derived from polyvinylidene chloride and activated at 750 and 850 C in carbon dioxide. The capacitance versus frequency plot, Figure 11, for these electrodes shows steeper slopes, about -1, than any other carbons tested, which again suggests the presence of a resistive film at the outer surface of the porous material.

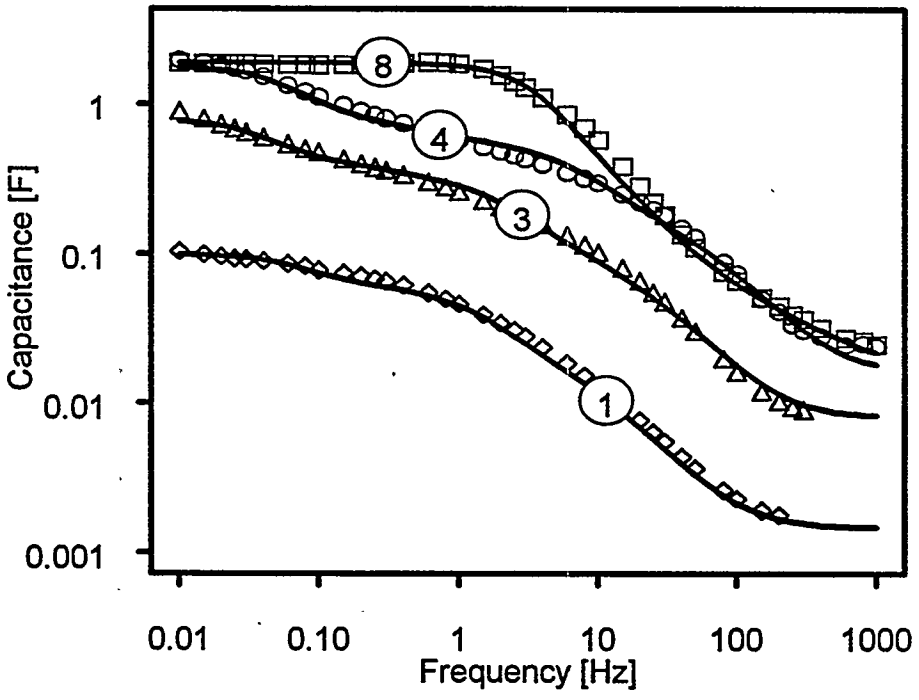

Figure 8: Frequency dependence of polyimide-derived carbon films, activated in 1, 3, 4 and 8 increments. For visual comparison, lines have been drawn through data points as derived from the transmission line equivalent circuit. These lines are not maximum-likelihood approximations.

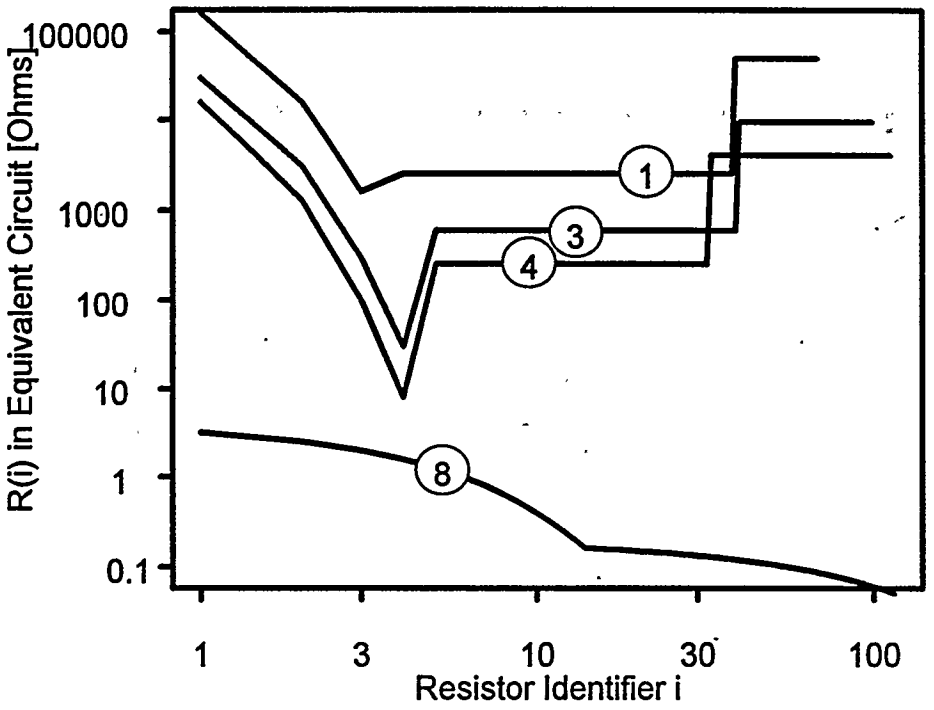

Figure 9: Resistance distribution for equivalent circuit to model the data in Figure 8.

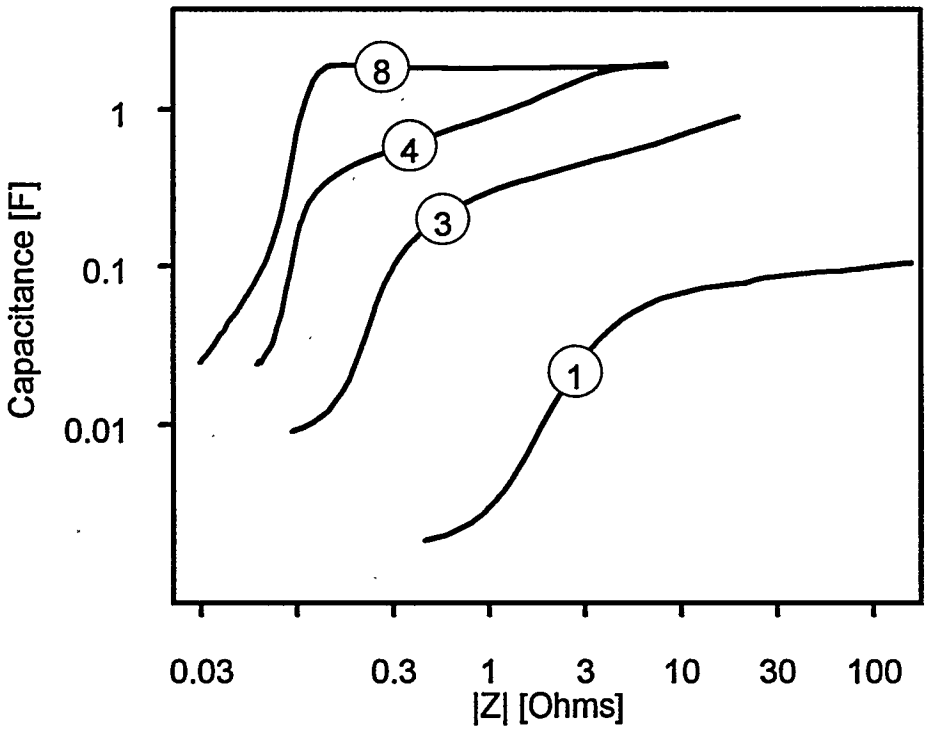

Figure 10: Impedance dependence of the capacitance of polyimide-derived carbon films.

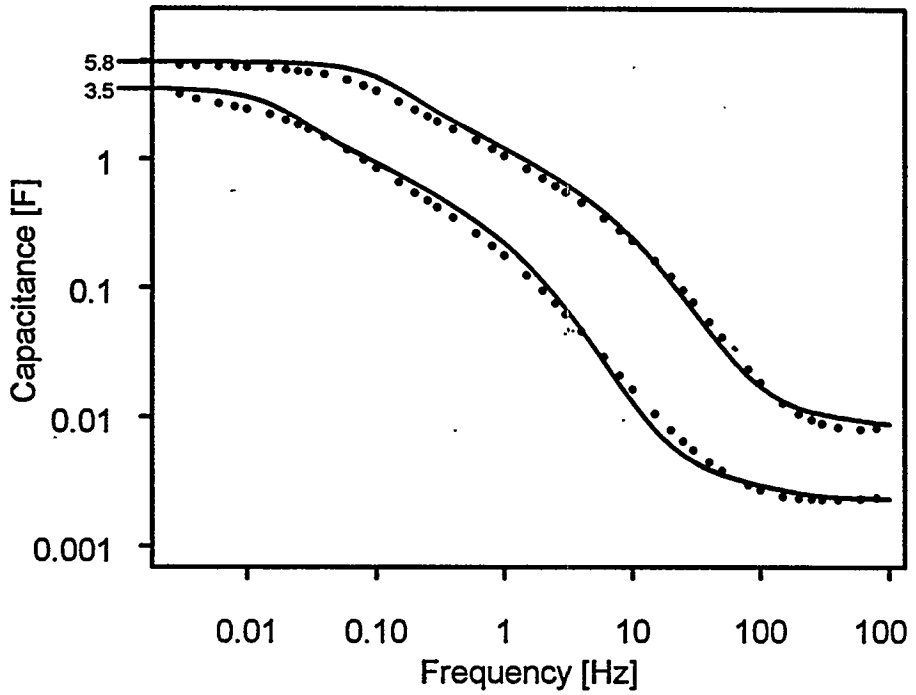

Figure 11: Frequency response curves for the capacitance of polyvinylidene chloride-derived carbon samples, activated in carbon dioxide at 850 (top curve) and 750 C.

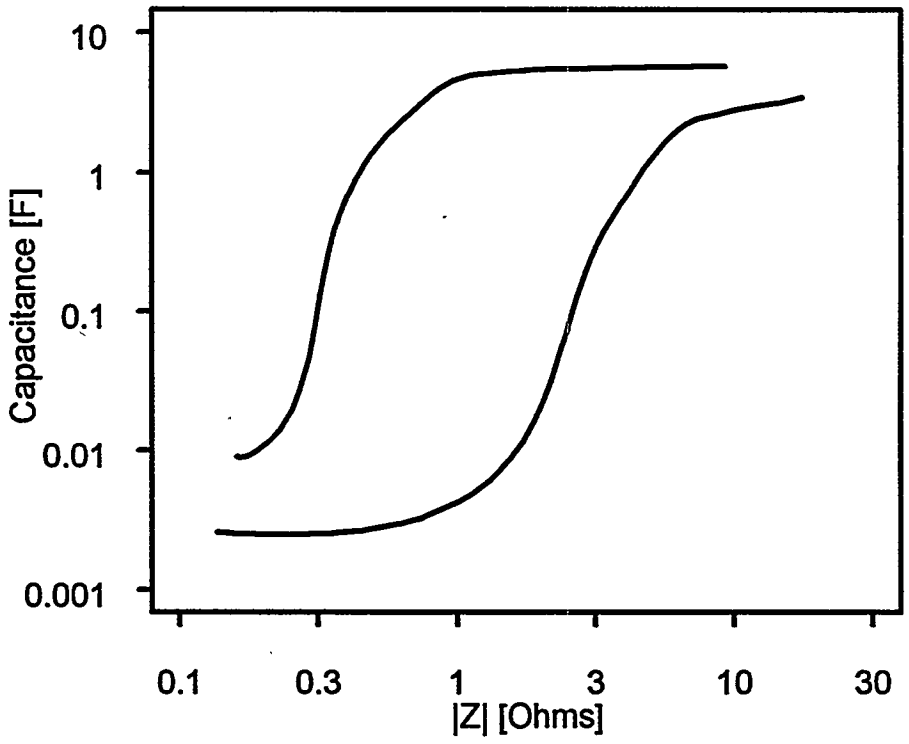

Figure 12: Impedance dependence of the capacitance of the same polyvinylidene chloride-derived carbon samples as characterized in Figure 11. (Top curve is for 850 C activation.)

Figure 12 presents the corresponding capacitance versus |Z| plot, which yields exceptionally high capacitance cutoff times. Table 1 summarizes the operating and performance data of the capacitors and capacitor materials used in this study. Small values for t_d in the last column suggest high power per stored energy, and are, therefore, indicative of superior material properties.

Table 1: Capacitor Sample Characterization

Sample Identification	Maximum Operating Voltage [V]	Capacitance at low Frequency [F]	Cutoff Time t_{cutoff} [sec]
Soleq 470	2.3	322	3.7
Soleq 70	3.5	55	1.65
Maxcap 1	5.5	0.76	0.98
Maxcap .022	5.5	0.027	0.31
NEC .1	10.0	0.34	0.28
NEC .022	10.0	0.125	0.34
Polyimide 8	0.5	1.92	0.18
Polyimide 4	0.5	1.86	0.18
Polyimide 3	0.5	0.87	0.20
Polyimide 1	0.5	0.10	0.23
Polyvinylidene chloride 750	0.5	3.5	9.0
Polyvinylidene chloride 850	0.5	5.8	2.06

Summary and Discussion

Impedance tests of commercial DLCs and of carbon film electrode materials were carried out to assess the correlation between various porous structures and the frequency dependence of the capacitance. The observed responses were modeled with impedance calculations for a transmission line equivalent circuit. All commercial DLCs showed a decrease of the capacitance with increasing frequency, approximating a slope of -0.5 in double logarithmic diagrams. Steeper slopes were found to be typical for carbon film electrodes, with values near -1. This behavior can be emulated with a short sequence of high resistance values at the front end of the equivalent circuit, and has been interpreted as a resistive or low-porosity layer enveloping the porous electrode material. Such a layer can only degrade DLC performance and its removal offers a great potential to further improve the properties of carbon films.[5] Although activated carbon films already achieve higher energy densities for DLCs than any other carbon material, it seems quite clear that not having previously dealt with the resistive layer may have compromised their ultimate performance. Since the established activation process operates, preferentially, in the interior of the porous structure, too much of the resistive surface remains. If instead the outer surface is removed first, then less activation will be necessary and the mechanical integrity of the material will be better preserved. Electrochemical surface accessibility

would improve, and energy density may still further increase. More importantly, power performance may significantly improve. A time variable, which correlates with the power-to-energy performance ratio of a capacitor, was derived from the absolute magnitude of the impedance and the capacitance at low frequency. Plots of the capacitance versus this variable exhibit cutoff characteristics ranging from 0.2 to 9 seconds, with smaller values indicating higher power-to-energy performance. Polyimide-derived carbon appears at the low end of this range, polyvinylidene chloride-derived carbon at the high end, and all commercial DLCs in-between.

Acknowledgment

David Ingersoll permitted access to his impedance test equipment and provided much appreciated advice.

References

[1]E. J. Dowgiallo and A. F. Burke, "Ultracapacitors for Electrical and Hybrid Vehicles-A Technology Update," Proceedings of the 11th International Electric Vehicle Symposium, Florence, Italy, 27-30 September 1992.

[2]E. T. Eisenmann, "Design Rules and Reality Check for Carbon-Based Ultracapacitors", Sand95-0671, April 1995.

[3] A. F. Burke and E. Blank, "Electric/Hybrid Transit Buses Using Ultracapacitors", paper presented at Mass Transit System Compatibility '95, Long Beach, California, September 1995.

[4]H. Keiser, K. D. Beccu and M. A. Gutjahr, "Abschätzung der Porenstruktur Poröser Elektroden aus Impedanzmessungen" Electrochimica Acta **21**, 539-543 (1976).

[5]E. T. Eisenmann, "New Carbon Activation Process for Increased Surface Accessibility in Electrochemical Capacitors," SAND94-1522

[6]W. R. Even, Sandia National Laboratories, California, Org. 8716, personal communication.

Unlimited Release
Initial Distribution

B. M. Barnett
Arthur D. Little, International
Acorn Park
Cambridge, MA 02140-2390

P. Davis
USDOE / Forestall Bldg / EE321
1000 Independence Ave SW
Washington, DC 20585

A. F. Burke
University of California, Davis
Davis, CA 95616

D. A. Evans
The Evans Company
33 Eastern Avenue
East Providence, RI 02914

J. R. Miller
JME, Inc.
17800 Parkland Drive
Shaker Heights, OH 44177

T. C. Murphy
INEL
PO Box 1625
Idaho Falls, ID 83415-3830

1	MS-0953	W. E. Alzheimer, 1500
1	MS-0613	D. H. Doughty, 1521
1	MS-0614	N. H. Clark, 1522
1	MS-0614	D. E. Mitchell 1522
1	MS-0614	R. K. Grothaus, 1523
1	MS-0614	N. Doddapaneni, 1523
20	MS-0614	E. T. Eisenmann, 1523
1	MS-0614	R. A. Guidotti, 1523
1	MS-0614	S. N. Hoier, 1523
1	MS-0614	D. Ingersoll, 1523
1	MS-0614	B. Johnson, 1523
1	MS-0614	G. Nagasubramanian, 1523
1	MS-0613	P. C. Butler, 1525
1	MS-0613	J. M. Freese, 1525
1	MS-0985	M. W. Callahan, 2602
1	MS-0560	P. A. Longmire, 5407
1	MS-9401	C. W. Robinson, 8702
1	MS-9404	J. C. F. Wang, 8713
1	MS-9404	J. M. Hruby, 8716
1	MS-9404	W. R. Even, Jr., 8716
1	MS-9404	M. X. Tan, 8716
1	MS-9018	CTF, 8523-2
5	MS-0899	Technical Library, 13414
1	MS-0619	Print Media, 12615
2	MS-0100	Document Processing, 7613-2 for DOE / OSTI

Org.	Bldg.	Name	Rec'd by	Org.	Bldg.	Name	Rec'd by

Sandia National Laboratories